A numerical investigation of structure–property relations in fibre composite materials

V. Sansalone [1], P. Trovalusci [2 *]

Abstract

A multifield continuous model is adopted to investigate the mechanical behaviour of heterogeneous materials made of short, stiff and tough fibres embedded in a more deformable matrix. This continuum accounts for the presence of internal structure by means of non-standard field descriptors. The constitutive relations, obtained by a multiscale approach linking the material description at different scales, depend on the geometry and the arrangement of the internal phases and include internal scale parameters, which allow taking into account size effects. A multiscale finite element technique has been used for obtaining the numerical solution of the multifield and the corresponding Cauchy model. The numerical results obtained on a sample fibre reinforced composite show the effectiveness of the former in pointing out the influence of the size, the shape and the orientation of the fibres on the gross behaviour of the material.

Keywords: Microstructure; Micropolar continua; Multiscale modelling; Composite materials; Homogenization; Finite element method.

Introduction

The continuous development of engineering applications requires more and more high-performance materials which show, at finer scales, various kinds of heterogeneities. Among them, polyphase metallic alloy systems, polymer blends, polycrystalline, textured media, fibre-matrix composites, biocomposite materials, up

*Corresponding author
[1]Lab. de Biomécanique et Biomatériaux Ostéo-Articulaires, CNRS UMR 7052, Université Paris 12.
61, Av. du Général de Gaulle, 94010 Créteil Cedex, France.
E-mail: vittorio.sansalone@univ-paris12.fr
[2]Dip. di Ingegneria Strutturale e Geotecnica, Università La Sapienza.
Via Gramsci 53, 00197 Roma, Italy.
E-mail: patrizia.trovalusci@uniroma1.it

to masonry-like materials. In the present work, we focus on a specific type of microstructured materials, namely fibre reinforced composites, which are characterized by the presence of stiff fibres embedded in a more deformable matrix.

Real world applications cannot afford a detailed description of the materials at the scale of the heterogeneities, but need effective *macroscopic* models capable to effectively describe the complex *microscopic* structure. A basic problem in the formulation of such models is to filter enough information to provide an accurate global description of the actual microstructure and of the mechanical phenomena occurring at that scale. Most part of the classical homogenized models [1, 2] are standard Cauchy continua that exhibit two major drawbacks. First, due to the absence of scale parameters, they make it impossible to distinguish the behaviour of materials made of particles of different size. Second, these models turn out to be not suited for the study, even in an elastic regime, of problems with geometric and loading singularities involving high stress and strain gradients [3]. The main difficulties arise when the characteristic size of the body is of the same order of magnitude of the size of the internal heterogeneities.

Different models have been proposed in order to avoid the above mentioned difficulties. Most of them can be seen as enhanced Cauchy continua where the microstructure is accounted for by means of internal parameters or higher order gradients of the displacement field [4, 5, 6].

The model adopted in this work is a micropolar continuum of the kind proposed in [7, 8] and relies on the theory of multifield continua [9]. In this framework, material particles are described, besides their position, by a number of additional parameters representing some kind of granularity, i.e. the local structure. In this case, the local structure is rigid and the additional parameters account for the fibres orientation. A key feature of such continua is that the new parameters are considered as observable variables, which must satisfy proper balance equations, and are thermodinamically consistent [10].

The constitutive relations are derived by following the multiscale strategy proposed in [11]. The micro–macro scale transition is effected by identifying a representative volume element (RVE) of the composite material, and therein defining the expression of the stored energy function. For a fibre composite material, we identify the RVE with the periodic module of a lattice model and the stored energy sums up the strain potential of the interactions between the elements of the lattice. Working in the same conceptual framework of the classical molecular theory of elasticity [12, 13], the strain energy of the continuum macromodel is then obtained by assuming homogeneous deformations in the discrete micromodel. In this way, the explicit expressions of the constitutive functions for both the standard and non-standard stress measures are derived. In this framework, empirical information must be only provided at the microscale, where the material response should be more easily described than at the macroscale. In order to make a comparison, the Cauchy continuum corresponding to the same micromodel with proper internal constraints, is also derived.

The described model has been implemented in a computer code, written in Object Oriented C++, designed in such a way to reflect as close as possible the multifield–multiscale nature of the model [8].

With reference to a target fibre reinforced composite material, some numerical simulations have been performed to investigate the effectiveness of the multifield model in accounting for the presence of the material microstructure. Results obtained for a sample system under various loading conditions allowed to examine some basic structure–property relations, such as the influence of the size and the orientation of the fibres on the gross behaviour of the material. Moreover, a comparison with the corresponding Cauchy model pointed out the improvement provided by the multifield model in describing the mechanical response of the system.

The outline of the paper is the following: first, in section 1 we will describe the multiscale procedure used for setting up the multifield model; then, in section 2, we will sketch the basic ingredients of the software developed to implement this model; finally, in section 3 we will go inside the structure–property relation, showing how a macroscopic property (deformability) depends on the microscopic structure (orientation and size of the fibres).

1 The multifield–multiscale model

Our reference material is a fibre reinforced composite characterized, at the microscopic level, by short, stiff fibres embedded in a deformable matrix. We assume perfect adhesion between the fibres and the matrix. Such a microscopic description applies to many real materials, such as fibre reinforced polymers (e.g. epoxy resin or other thermoset polymer matrix reinforced with glass or carbon fibres [14]), masonry-like materials with stone/bricks embedded in a mortar matrix [11], as well as many biomaterials (e.g. nacre or bones microstructure [15]).

At the macroscopic level, such a composite material is described in terms of a generalized multifield continuum, whose constitutive response is obtained by a multiscale procedure bridging the macroscopic averaged response to the actual microscopic state. The framework of this formulation has been set forward in [3] and here we recall only its basic ingredients. Moreover, even if the procedure is quite general, in the following we will restrict our attention to the case of short-fibre composites.

The multifield continuum model, the *macromodel*, is built up based on the mechanics of a suitable lattice model, the *micromodel*, made of interacting rigid particles, representing the fibres in the matrix [7, 14]. Considering materials with periodic microstructure, a representative volume element, in the following referred to as *module*, can be defined, describing the internal material texture. The procedure governing the scale transition between the micromodel and the macromodel is based on two key assumptions, standard in the classical molecular theory of elasticity [12, 13]:

(a) the admissible deformations for the module are considered homogeneous;

(b) the volume average of the strain energy of the module, ϕ_μ, is equated to the strain energy density of the macromodel, ϕ_M.

In particular, assumption **(b)** points out our conceptual framework, inspired by Voigt's work [12] and aiming at building up a suitable energy form at the macroscale.

Assuming a linearized kinematics, the meaningful strain measures of the module are: the relative displacement between two points, p^{a} and p^{b}, belonging to two particles, A and B, centred at the positions a and b, represented by the vector $\mathbf{u}^{\mathsf{ab}} = \mathbf{u}^{\mathsf{a}} - \mathbf{u}^{\mathsf{b}} + \mathrm{W}^{\mathsf{a}}\left(\mathsf{p}^{\mathsf{a}} - \mathsf{a}\right) - \mathrm{W}^{\mathsf{b}}\left(\mathsf{p}^{\mathsf{b}} - \mathsf{b}\right)$, where $\mathbf{u}^{\mathsf{a}}$ ($\mathbf{u}^{\mathsf{b}}$) is the displacement vector of a (b), and W^{a} (W^{b}) is the skew-symmetric tensor of the rotation of the particle A (B); and the relative rotation between two particles, represented by the skew-symmetric tensor $\mathrm{W}^{\mathsf{ab}} = \mathrm{W}^{\mathsf{a}} - \mathrm{W}^{\mathsf{b}}$.

The actions corresponding, in the sense of virtual work, to the above kinematical quantities are the force and the couple exchanged between A and B, represented by the vector $\mathbf{t}^{\mathsf{ab}}$ and the skew-symmetric tensor C^{ab}, respectively.

It follows that the mean strain energy over the module of volume V reads

$$\phi_\mu = \frac{1}{2V}\sum_{\mathsf{ab}}\left\{\mathbf{t}^{\mathsf{ab}}\cdot\left[\mathbf{u}^{\mathsf{ab}} - \mathrm{W}^{\mathsf{a}}\left(\mathsf{p}^{\mathsf{a}} - \mathsf{p}^{\mathsf{b}}\right)\right] + \frac{1}{2}\mathrm{C}^{\mathsf{ab}}\cdot\mathrm{W}^{\mathsf{ab}}\right\}. \tag{1}$$

By considering homogeneous deformations for the module (hypothesis **(a)**), the displacement and rotation of the fibres can be expressed as

$$\begin{array}{rcccl} \mathbf{u}^{\mathsf{a}} & = & \boldsymbol{u}\left(\mathsf{x}\right) & + & \nabla\boldsymbol{u}\left(\mathsf{x}\right)\left[\mathsf{a}-\mathsf{x}\right], \\ \mathrm{W}^{\mathsf{a}} & = & W(\mathsf{x}) & + & \nabla W(\mathsf{x})\left[\mathsf{a}-\mathsf{x}\right], \end{array} \tag{2}$$

where $\boldsymbol{u}$ and W are regular fields defined on a continuum neighbourhood centred at x, representing the standard displacement vector field and the microrotation skew-symmetric tensor field, respectively. We point out that the limitation of assumption **(a)** relies in its capability to describe the actual microstructural state. When the characteristic wave length of phenomena is smaller of or even comparable to the microstructural characteristic length, such an assumption may not hold any more. Anyway, our model introduces an affine expansion for both displacement and microrotation of the fibres. In this way, it behaves like a second-order Cauchy model and can represent localization phenomena much better than the first-order Cauchy model [14].

Using Eqs. (2) it is possible to show [7] that the corresponding macroscopic model comes out to be a Cosserat continuum [16], whose strain energy density reads

$$\phi_M = \frac{1}{2}\left\{S\cdot\left(\nabla\boldsymbol{u} - W\right) + \frac{1}{2}\boldsymbol{S}\cdot\nabla W\right\}. \tag{3}$$

The generalized Cauchy stress field S and the couple-stress third order tensor field $\boldsymbol{S}$ are identified in terms of the internal actions of the module and of the geometry of the microstructure, leading to:

$$\begin{array}{rcl} S\left(\mathsf{x}\right) & = & \dfrac{1}{V}\left\{\displaystyle\sum_{\mathsf{ab}}\mathbf{t}^{\mathsf{ab}}\otimes\left(\mathsf{a}-\mathsf{b}\right)\right\}, \\ \boldsymbol{S}\left(\mathsf{x}\right) & = & \dfrac{1}{V}\left\{\displaystyle\sum_{\mathsf{ab}}2\mathbf{t}^{\mathsf{ab}}\otimes\left(\left(\mathsf{p}^{\mathsf{a}}-\mathsf{a}\right)\otimes\left(\mathsf{a}-\mathsf{x}\right) - \left(\mathsf{p}^{\mathsf{b}}-\mathsf{b}\right)\otimes\left(\mathsf{b}-\mathsf{x}\right) - \left(\mathsf{p}^{\mathsf{a}}-\mathsf{p}^{\mathsf{b}}\right)\otimes\left(\mathsf{a}-\mathsf{x}\right)\right)\right. \\ & + & \left.\displaystyle\sum_{\mathsf{ab}}\mathrm{C}^{\mathsf{ab}}\otimes\left(\mathsf{a}-\mathsf{b}\right)\right\}. \end{array} \tag{4}$$

Quite interestingly, Eq. (4a) is precisely the *Virial formula* used at the atomic scale in calculating stresses from molecular positions and interatomic forces.

After assigning constitutive relations for the internal actions of the module:

$$\mathbf{t}^{\mathsf{ab}} = \boldsymbol{\mathcal{F}}_{\mathbf{t}} \left(\mathbf{u}^{\mathsf{ab}}, \mathrm{W}^{\mathsf{ab}}\right) , \quad \mathrm{C}^{\mathsf{ab}} = \boldsymbol{\mathcal{F}}_{\mathrm{C}} \left(\mathbf{u}^{\mathsf{ab}}, \mathrm{W}^{\mathsf{ab}}\right) , \tag{5}$$

and expressing the strain measures $\mathbf{u}^{\mathsf{ab}}$ and W^{ab} by means of Eqs. (2), the constitutive relations for the stress measures of the multifield continuum can be expressed in terms of the macroscopic kinematical fields:

$$S = \mathcal{F}_S \left(\nabla \boldsymbol{u} - W, \nabla W\right) , \quad \boldsymbol{S} = \mathcal{F}_{\boldsymbol{S}} \left(\nabla \boldsymbol{u} - W, \nabla W\right) . \tag{6}$$

In particular, if the constitutive relations for the micromodel are assumed to be linear elastic:

$$\mathbf{t}^{\mathsf{ab}} = \mathbf{K}_{\mathbf{t}}^{\mathsf{ab}} \, \mathbf{u}^{\mathsf{ab}} , \quad \mathrm{C}^{\mathsf{ab}} = \mathbf{K}_{\mathrm{C}}^{\mathsf{ab}} \, \mathrm{W}^{\mathsf{ab}} , \tag{7}$$

with $\mathbf{K}_{\mathbf{t}}$ and $\mathbf{K}_{\mathrm{C}}$ symmetric constitutive tensors of second and fourth order respectively, the stress–strain relations for the linear elastic anisotropic Cosserat continuum can be obtained by substituting Eqs. (2) into Eqs. (7) and the latter into Eqs. (4)

$$\begin{array}{rcl} S &=& \mathbf{A} \left(\nabla \boldsymbol{u} - W\right) \;+\; \mathbf{B} \, \nabla W , \\ \boldsymbol{S} &=& \mathbf{C} \left(\nabla \boldsymbol{u} - W\right) \;+\; \mathbf{D} \, \nabla W . \end{array} \tag{8}$$

The constitutive tensors $\mathbf{A}$, $\mathbf{B}$, $\mathbf{C}$, and $\mathbf{D}$ depend on the elastic constants of the matrix and on the geometry and arrangement of the fibres. In particular, the tensors $\mathbf{B}$, $\mathbf{C}$, and $\mathbf{D}$ depend on the size of the fibres, allowing to properly take into account size effects. Moreover, material hyperelasticity entails symmetry relations between the tensors $\mathbf{B}$ and $\mathbf{C}$. Finally, if fibres in the matrix are arranged according to central symmetry, as in the case of periodic microstructures, material indifference considerations imply the tensors $\mathbf{B}$ and $\mathbf{C}$ to be null.

1.1 The multiscale Cauchy model

The described multiscale strategy can also be used to identify the constitutive functions for the stress measure of an anisotropic Cauchy continuum. In this case, we assume that the rotation of each particle equals the local rigid rotation, which corresponds to impose to the module the internal constraint: [1]

$$W = \mathtt{skw} \nabla \boldsymbol{u} . \tag{9}$$

By posing $\mathrm{W} := W(\mathsf{x})$, it follows $\mathrm{W}^{\mathsf{a}} = \mathrm{W}$ for each particle A of the module, and the strain measures of the module reduce to $\mathbf{u}^{\mathsf{ab}} = \mathbf{u}^{\mathsf{a}} - \mathbf{u}^{\mathsf{b}} + \mathrm{W}[(\mathsf{p}^{\mathsf{a}} - \mathsf{p}^{\mathsf{b}}) - (\mathsf{a} - \mathsf{b})]$, while the only meaningful internal actions reduce to $\mathbf{t}^{\mathsf{ab}}$. In this setting, the mean strain energy of the constrained module becomes

$$\widehat{\phi}_{\mu} = \frac{1}{2V} \sum_{\mathsf{ab}} \mathbf{t}^{\mathsf{ab}} \cdot \left[\mathbf{u}^{\mathsf{ab}} - \mathrm{W} \left(\mathsf{p}^{\mathsf{a}} - \mathsf{p}^{\mathsf{b}}\right)\right] . \tag{10}$$

[1] `skw` is the linear operator selecting the skew-symmetric part of a second order tensor.

By substituting Eqs. (2) with the constraint (9) into Eq. (10), through hypothesis **(b)**, the strain energy density of the macromodel corresponds to the strain energy density of a Cauchy continuum

$$\widehat{\phi}_M = \frac{1}{2}\,\widehat{S}\cdot E, \tag{11}$$

where $E = \mathtt{sym}\nabla\boldsymbol{u}$.[2] Constitutive identification of the Cauchy stress $\widehat{S}$ results in:

$$\widehat{S}\,(\mathsf{x}) = \frac{1}{V}\,\mathtt{sym}\sum_{ab}\mathbf{t}^{\mathsf{ab}}\otimes(\mathsf{a}-\mathsf{b})\,. \tag{12}$$

By assuming linear microscopic constitutive prescriptions, Eqs. (7a), the stress–strain relation for the Cauchy continuum reads:

$$\widehat{S} = \widehat{\mathbf{A}}\,E\,. \tag{13}$$

The constitutive tensor $\widehat{\mathbf{A}}$ depends only on the shape, the orientation and the arrangement of the fibres, but not on their size. This makes it impossible to describe by such a model any scale effect related to the actual size of the heterogeneities.

2 Some details on the multiscale procedure

A specific computer code, written in Object Oriented C++ language, has been set up in order to implement the multiscale multifield model described in the previous section. It allows for finite element analysis of plane elasticity problems in the presence of additional scalar or vector fields, besides the standard displacement one. A preliminary version of this code has been described in [8].

A Monte Carlo algorithm and a path-following algorithm have been implemented. A few template field models have been pre-designed and included, in order to deal with the most common field problems in the mechanics of materials. However, the structure of the code allows users to easily implement and study their own field problems.

The main feature of this code is the truly multiscale algorithm adopted to find the solution of the multifield problem. The same algorithm can be used to solve the classical problem. The scheme can be conceptually splitted into three steps:

- a localization step, Eqs. (2)
- the evaluation of micro-actions, Eqs. (5);
- a homogenization step, Eqs. (4) or (12).

In this way, by proper definition of suitable response functions for the microscopic internal actions, $\mathbf{t}^{\mathsf{ab}}$ and C^{ab}, the procedure can easily take into account different constitutive behaviours. In fact, in order to compute the macroscopic stress, S and $\boldsymbol{S}$, the multiscale scheme resorts directly to Eqs. (4), which do not explicitly depend

[2] `sym` is the linear operator selecting the symmetric part of a second order tensor.

on the microscopic constitutive law, but are defined only in terms of the micro-actions $\mathbf{t}^{\mathsf{ab}}$ and C^{ab}. In turn, these micro-actions are computed at the microscopic level by means of Eqs. (5) starting from the kinematics described by Eqs. (2). In this way, it is possible to take automatically into account any microscopic nonlinear constitutive relation, without resorting to complex calculations in order to obtain a macroscopic nonlinear constitutive law.

3 Numerical simulations

In the following, we will show the capability of the multifield model described in Section 1 in studying the relation between the microstructural features and the macroscopic elastic properties of a system. Moreover, results are compared with those obtained by the corresponding anisotropic Cauchy model, as described in Section 1.1. We will restrict our attention to a simplified setting: besides the already mentioned hypothesis of linearized kinematics, the matrix is assumed to be linearly elastic and isotropic, i.e., characterized by the Young modulus E and the shear modulus G. Nevertheless, as long as small deformations are concerned, these hypoteses, together with that of rigid fibres, effectively applies to a wide class of real composite materials.

In Section 3.1 we will discuss the specific material identification in further details. In Section 3.2 we will finally go inside the structure–property relation, showing how a macroscopic property (deformability) depends on the microscopic structure (orientation and size of the fibres).

3.1 Material identification

At the microscopic level, we consider the module depicted in Fig. 1 by the light shaded area. Each module fills the entire space by periodic translation. The fibres, represented by the dark shaded rectangles in the figure, are embedded in a volume of size $w\,t$. This volume element, referred to as *block*, is the smallest unit explicitly represented by its center of mass. To describe the interactions between fibres we consider linearly elastic springs, referred to as *joints*, along the contact surfaces between blocks. The springs, represented by thick segments in the figure, are the only deformable elements and describe the effect of the matrix. Their stiffness, Eqs. (7), is expressed as

$$\begin{array}{rcl} \mathbf{K}_{\mathbf{t}}^{\mathsf{ab}} & = & \mathbf{K}_{\mathbf{t}}^{\nu\nu}\,\nu\otimes\nu + \mathbf{K}_{\mathbf{t}}^{\tau\tau}\,\tau\otimes\tau\,, \\ \mathbf{K}_{\mathrm{C}}^{\mathsf{ab}} & = & \mathbf{K}_{\mathrm{C}}^{\nu\tau\nu\tau}\left(\nu\otimes\tau\otimes\nu\otimes\tau - \tau\otimes\nu\otimes\tau\otimes\nu\right)\,, \end{array} \tag{14}$$

where ν and τ refer to the direction parallel and orthogonal to the spring axis, respectively. The coefficients $\mathbf{K}_{\mathbf{t}}^{\nu\nu}$, $\mathbf{K}_{\mathbf{t}}^{\tau\tau}$ and $\mathbf{K}_{\mathrm{C}}^{\nu\tau\nu\tau}$ are identified on the basis of the morphology of the module and of the elastic moduli of the matrix.

With reference to the generic pair of fibres A and B, interacting through a joint of width w^{ab} and thickness t^{ab},[3] let α^{ν} and α^{τ} be coefficients accounting for the

[3]More precisely, w^{ab} and t^{ab} are the width and thickness of the part of matrix through the fibres A and B

effective width and thickness in computing the axial and tangential stiffness of the joint, respectively. Then

$$\mathbf{K}_{\mathbf{t}}^{\nu\nu} = E\,\frac{\alpha^{\nu}\,w^{\mathsf{ab}}}{t^{\mathsf{ab}}}\,, \qquad \mathbf{K}_{\mathbf{t}}^{\tau\tau} = G\,\frac{\alpha^{\tau}\,w^{\mathsf{ab}}}{t^{\mathsf{ab}}}\,, \qquad \mathbf{K}_{\mathrm{C}}^{\nu\tau\nu\tau} = \frac{1}{4}\mathbf{K}_{\mathbf{t}}^{\nu\nu}\,(\alpha^{\nu}\,w^{\mathsf{ab}})^2\,. \tag{15}$$

Note that such an identification is suitable when the effect of the matrix can be effectively described by a set of springs, that is when the distance between fibres is "small" enough. In particular, this means that the couple C^{ab}, exerted on fibre A by fibre B, is equal to the couple C^{ba}, exerted on fibre B by fibre A: that is, shear related variations of the value of such a couple, moving from A to B, are considered negligible.

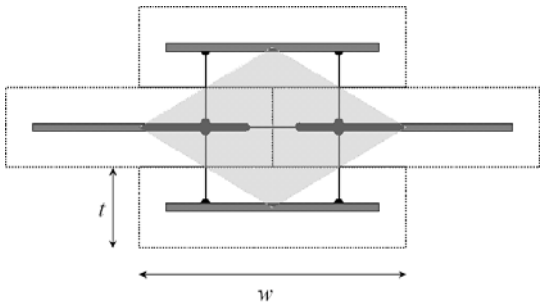

Figure 1: Sketch of the orthotropic lattice module adopted as microscopic model.

In this case, the module represents an orthotropic linear elastic material and the corresponding multifield material is an orthotropic Cosserat continuum whose costitutive relations are identified, as described in Section 1, in terms of the elastic constants (15) and the size and the arrangement of the fibres. The non null components of the costitutive tensors in Eqs. (8) are

$$\begin{array}{rclcrcl}
\mathbf{A}_{1111} &=& a_1\,G\,\rho^2 + a_4 E\,, & & \mathbf{A}_{1212} &=& 4a_1\,G\,, \\
\mathbf{A}_{2121} &=& a_2\,E\,\rho^2 + a_3 G\,, & & \mathbf{A}_{2222} &=& 4a_2\,E\,, \\
\multicolumn{7}{c}{} \\
\mathbf{D}_{121121} &=& \left(\frac{a_1}{4}\,G + (\frac{a_2}{16} + \frac{a_2^3}{4})\,E\,\rho^2 + a_4\,E\,\rho^{-2}\right)\,w^2\,, & & & & \\
\mathbf{D}_{122122} &=& a_1\,G\,t^2 + \frac{1}{4}(a_2 + a_2^3)\,E\,w^2\,, & & & &
\end{array} \tag{16}$$

where $\rho := w/t$ is the *aspect ratio* of the module, and a_i $(i = 1, 4)$ are the coefficients in Eqs. (15) evaluated for the "bed" and the "head" joints, namely: $a_1 = \alpha^{\tau}_{bed}$, $a_2 = \alpha^{\nu}_{bed}$, $a_3 = \alpha^{\tau}_{head}$ and $a_4 = \alpha^{\nu}_{head}$. Note that, being the module centrosymmetric, the tensors $\mathbf{B}$ and $\mathbf{C}$ in Eqs. (8) are null.

The non null components of the anisotropic Cauchy elastic tensor $\widehat{\mathbf{A}}$, Eq. (13), are

$$\begin{array}{rcl}
\widehat{\mathbf{A}}_{1111} &=& a_1\,G\,\rho^2 + a_3 E\,, \\
\widehat{\mathbf{A}}_{1212} &=& \widehat{\mathbf{A}}_{2121} = \frac{1}{2}\left(a_2\,E\,\rho^2 + (4a_1 + a_3)\,G\right)\,, \\
\widehat{\mathbf{A}}_{2222} &=& 4a_2\,E\,.
\end{array} \tag{17}$$

In the numerical simulations below our reference material is a polymer-matrix fibre composite, such as epoxy/glass. We will adopt the experimental values of

$E = 3.5\,\mathrm{GPa}$ and $G/E = 0.4$, common to epoxy and polyester. Both such thermo sets have an experimental value of Poissons ratio of $\nu = 0.25$, i.e., identical to the value $\nu_{iso} = E/2\,G - 1 = 0.25$ corresponding to an ideally isotropic material.

3.2 Macroscopic properties and microstructure

Our simulations refer to the 2-dimensional system shown in Fig. 2: a beam of length L (parallel to the X Cartesian axis) and height $H = L/10$ (parallel to the Y Cartesian axis), in plane-strain, constant-force loading condition. Three types of loading tests will be simulated: (1) traction, represented by a symmetric tensile loading at both ends of the beam (Fig. 2a); (2) shear, represented by two equal and opposite loadings at the two ends of the beam (Fig. 2b); (3) four-point bending, represented by two point loads applied on the top side, at a distance $L/3$ and $2\,L/3$ along the beam, while the two ends are held fixed at the bottom side (Fig. 2c). In all cases, the applied force is such that the maximum displacement is within 2-3% of L, so making satisfactory the hypothesis of linearized kinematics.

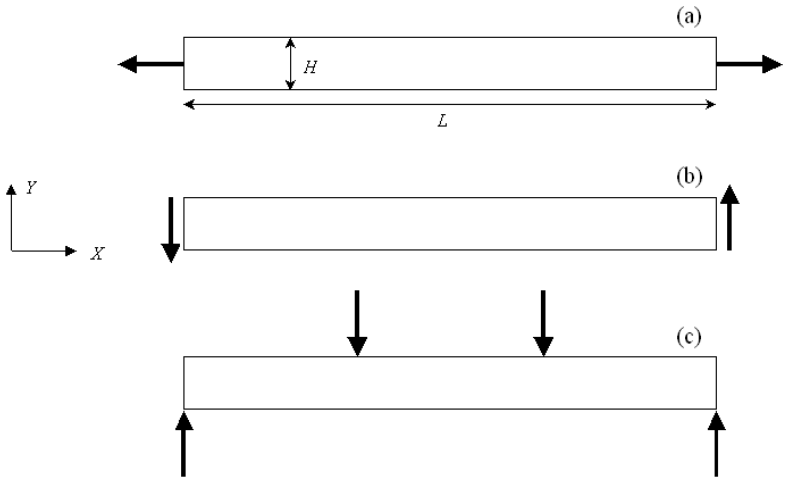

Figure 2: Sketch of the simulated system, a beam of length L and heigth $H = L/10$. Loading cases: (a) traction test; (b) shear test; (c) 4-point bending test.

As macroscopic property, we will focus on the deformability of the structure. A suitable measure of the deformability is the total deformation energy stored in the system, i.e., the strain energy density integrated over the volume V of the beam. In fact, the simulations being performed in constant force condition, the larger the stored deformation energy, the larger are the displacements involved.

All the results will be presented as a function of the *scale factor* $\lambda := w/L$, representing the size of the module compared with the size of the system, and of the (initial) *fibre orientation* φ, that is the orientation of the module with respect to an external reference system, which in our simulations is depicted in Fig. 2. In particular, $\varphi = 0$ indicates fibres parallel to the X-axis of the system. In the present work, we will not concern ourselves with the effect of the aspect ratio of the module, which is kept fixed: $\rho = 10$.

In the following figures, unless differently stated, solid lines will refer to the multifield (MF) model while dashed lines to the anisotropic Cauchy (AC) model.

Deformability vs. fibre orientation φ

Fig. 3 describes how the deformability of the system depends on the initial fibre orientation φ. First, second and third rows refer to traction, shear and bending tests, respectively. In the left column plots, the strain energy of the MF model, $\Phi_{\mathrm{MF}} := \Phi_M = \int_V \phi_M$, is plotted as a function of the initial fibre orientation φ, for different values of λ ranging from 1.0×10^{-2} to 1.0×10^{-4} (for smaller values of λ, results become indistinguishable from each other). In the same figure, dashed curves represent the corresponding AC model, $\Phi_{\mathrm{AC}} := \widehat{\Phi}_M = \int_V \widehat{\phi}_M$. As it will be thoroughly discussed in next session, for each loading test the AC response is described by a single curve, independently of the value of λ assumed in the simulation. The Φ_{MF} and Φ_{AC} curves are scaled by the value Φ_{C} corresponding to the φ- and λ-independent, isotropic Cauchy model (matrix without fibres).

It is clear that the response of both the MF and AC model strongly depends on the initial fibre orientation: in both cases, the deformability of the structure increases as the fibre orientation moves from 0 to $\pi/2$. The response of the two models is close, or even equal, while φ approaches 0 or $\pi/2$ (for the traction test, the two models provide exactly the same solution at $\varphi = 0, \pi/2$). However, very large differences are seen at any intermediate value of φ, the maximum discrepancy always occurring around $\varphi = \pi/4$ (see the plots in the right column in Fig. 3). Anyway, for all the considered values of λ, the MF model appears to describe a less rigid composite than the corresponding AC model, since the total strain energy stored in the former, Φ_{MF}, is always higher than in the latter, Φ_{AC}.

For the traction test, the response of the MF model is independent of λ and all the curves are superimposed. This will be thoroughly discussed in the next section.

The stored strain energy provides a synthetic measure of the deformability of the system, but cannot point out localized differences in the response of the MF and AC model. In order to do that, it is necessary to look at the pointwise description of the various fields provided by the two models.

A meaningful piece of information is given in Fig. 4, where we show a detailed picture of the fibre rotation depicted by both the multifield ($\lambda = 4.0 \times 10^{-3}$) and the Cauchy model in the 4-point bending test. The suitable descriptor in the MF model is the microrotation field, W, actually representing the rotation of the fibres (Eq. 2b), or more precisely its unique independent component, namely W_{21}. In the AC model the fibres are constrained to follow the macroscopic rotation, so the appropriate kinematical descriptor is the unique independent out-of-diagonal component of the skew-symmetric part of the displacement gradient, namely $\mathtt{skw}\,(\nabla \boldsymbol{u})_{21}$. Once again, the AC model comes out to be much stiffer than the MF. It is unable to describe high microrotation gradients, as in the regions close to the points where loads are applied: in fact, the fibre rotation realized in the MF model is always much higher than in the AC. For $\varphi = 0$, when the two models show a similar deformability in terms of stored strain energy, the difference in the value of the local fibre rotation is as large as +20% near the loading points, +50% near the ends. For

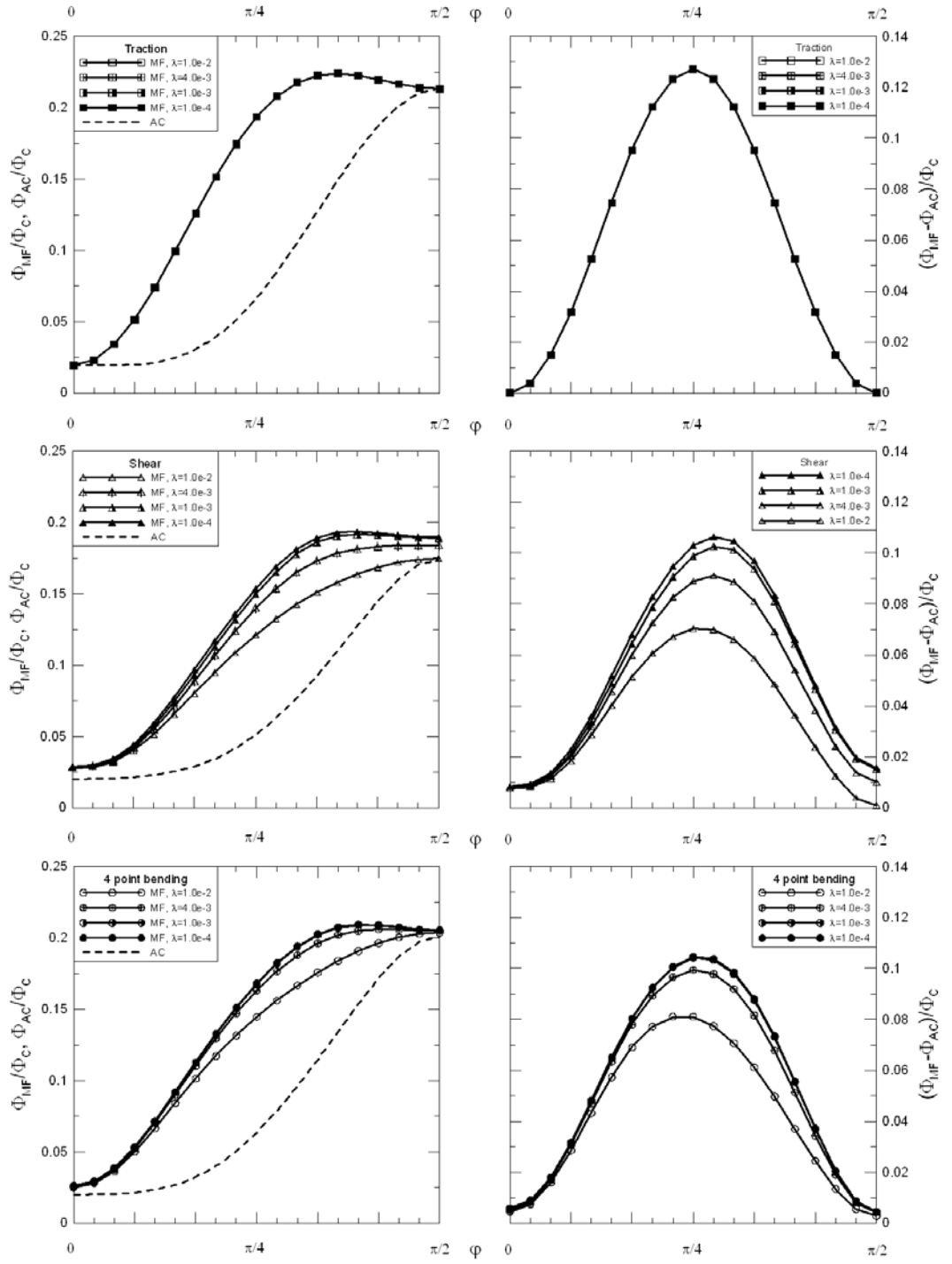

Figure 3: Deformability vs. fibre orientation φ: (a) traction; (b) shear; (c) bending. On the left: total strain energy for the multifield, Φ_{MF}, and the anisotropic Cauchy, Φ_{AC}, models. On the right: difference between the two models.

$\varphi = \pi/4$ the two models provide a completely different representation of the fibre rotation field, and the value at the ends provided by the MF model is three times larger than that of the AC. It must be pointed out that such results hold for the chosen value of λ, since the MF response strongly depends on it.

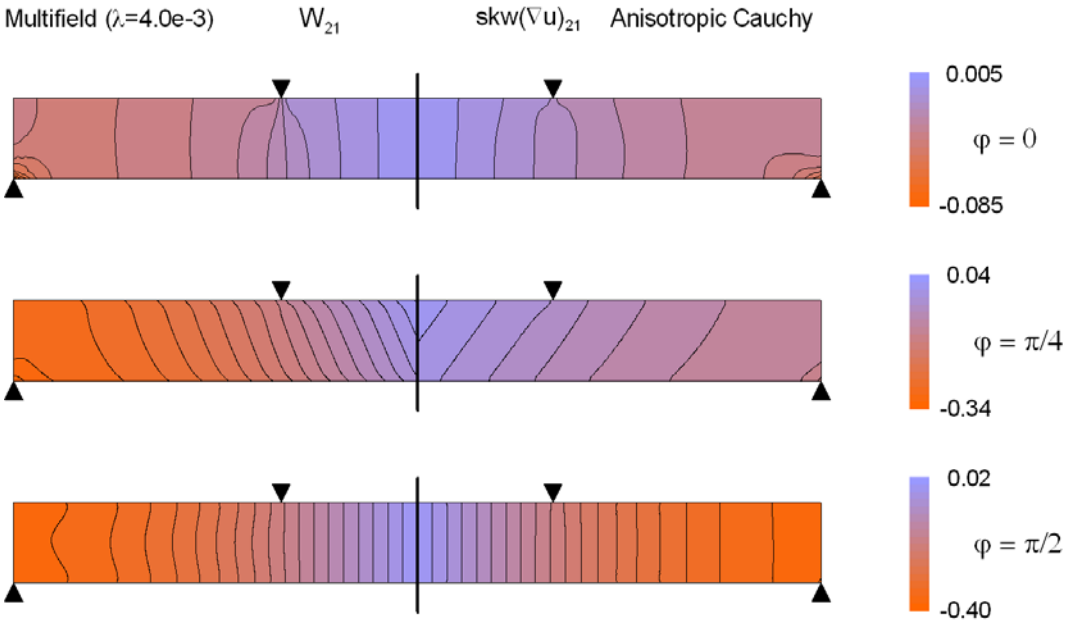

Figure 4: Contour map of the fibre rotation. On the left: multifield model ($\lambda = 4.0\times10^{-3}$), map of the microrotation field. On the right: anisotropic Cauchy model, map of the skew-symmetric part of the displacement gradient (macrorotation).

Deformability vs. scale factor λ

One of the main features of the multifield model is its ability to describe the dependency of the macroscopic response on the size of heterogeneities. In a linearized setting, this is clear from Eqs. (16), where the size of the module, w, enters the expression of constitutive coefficients $\mathbf{D}_{121121}$ and $\mathbf{D}_{122122}$. On the contrary, the response of the AC model does not depend on the size of the heterogeneities, since none of the coefficients $\widehat{\mathbf{A}}_{ijhk}$ does, Eqs. (17).

The appearance of an intrinsic scale length in the MF model is clearly shown in Fig. 5, in which the strain energy is reported as a function of the scale factor λ, for different values of φ. In the same figure, dashed straight lines represent the results obtained for the AC model, which clearly do not depend on λ. On the other hand, this is apparent also in the left plots of Fig. 3, where the AC response is represented by a single dashed curve.

Fig. 5 shows one of the main differences between the MF and the AC model. The latter cannot describe local rotations of the fibres inside the module, and therefore it is unable to describe size effects in the material response. On the contrary, the multifield model can represent different rotations of the fibres inside the module

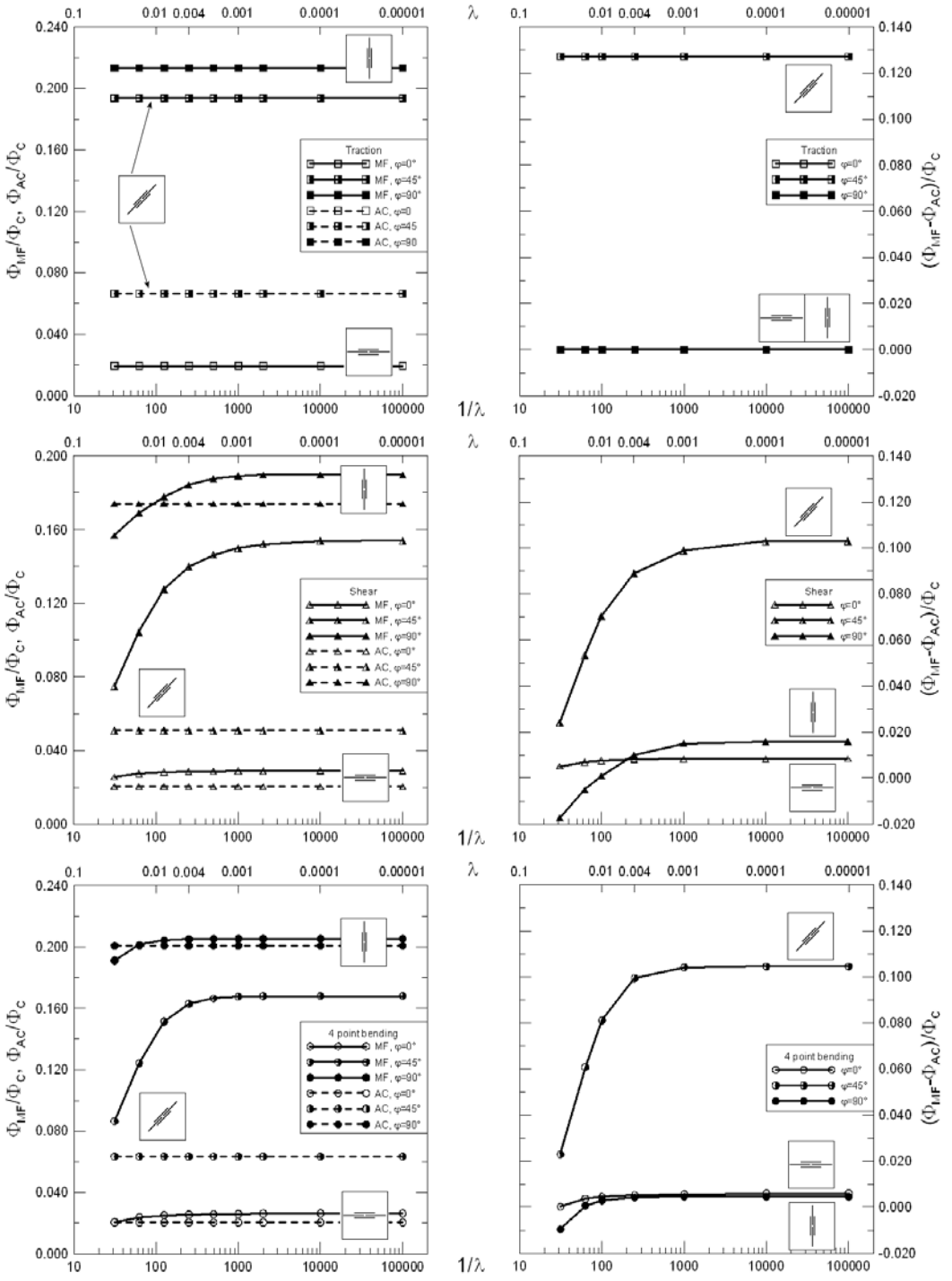

Figure 5: Deformability vs. scale factor λ: (a) traction; (b) shear; (c) bending. On the left: total strain energy for the multifield, Φ_{MF}, and the anisotropic Cauchy, Φ_{AC}, models. On the right: difference between the two models.

and explicitly takes into account the size of the module in the constitutive relation, Eqs. (16), and thus it is able to catch the dependency of the material response on the scale parameter λ.

As hinted in the previous section, in the traction test the response of the MF model is independent of λ and, for each value of φ, it is represented by a straight line (plots in the first row of Fig. 5). In fact, for the specific loading condition, the solution is characterized by $W = \texttt{const}.$ and therefore it is not affected by the size of the module, which enters only the constitutive coefficients related to ∇W. Nevertheless, the MF response is in general different from that of the AC model: only for $\varphi = 0, \pi/2$ the two solutions coincide, since in this case it turns out that $W = 0$.

The plots referring to the shear and 4-point bending test (second and third row in Fig. 5) show that, when λ decreases, the response of the MF model approaches an asymptotic value. That means that, from a certain value of $1/\lambda$ on (that is, when the size of the microstructure decreases under a certain value), there is no difference in the macroscopic response. Anyhow, in general, this asymptotic value remarkably differs from that, λ-independent, shown by the AC model. On the contrary, the MF response sharply varies when the size of heterogeneities increases. It must be pointed out that for smaller values of $1/\lambda$, when the size of the heterogeneities approaches the size of the system, hypothesis **(a)** in Section 1 is less and less satisfied and the solution looses reliability. In any case, the main discrepancy between the two models is generally observed for $\varphi = \pi/4$.

4 Final remarks

In this work some applications of a recently developed multifield–multiscale continuum model [11, 8, 14] have been presented, in order to study how the macroscopic response of a fibre reinforced composite material is influenced by the actual microscopic features.

A suitable finite element computer code has been written in order to implement the model, which can solve quasi-static equilibrium problems for continuous bodies characterized by a nonlinear material response. The code has been designed in such a way to reflect as close as possible the multifield–multiscale nature of the problem.

As target material, we considered a composite made of a deformable epoxy matrix reinforced with short, stiff glass fibres. We studied a sample system corresponding to a beam under traction, shear and 4-point bending loading conditions. Simulations have been performed under the hypothesis of linearized kinematics and assuming linearly elastic constitutive laws for the actions at the micro-scale.

Analysis of the numerical results clearly demonstrated the ability of the multifield continuum in pointing out the influence of the microstructural features (size of the heterogeneities, arrangement of the fibres) on the macroscopic response. Furthermore, some local details of the global response (e.g., high gradients of the fields near the loading points) are well described. The quality of the solution is even more apparent if compared with that of the classical anisotropic Cauchy continuum, which provides a much stiffer response and is completely unable to catch some key features

like the dependency of the macroscopic response on the size of the heterogeneities. It is worth noting that the quality of the results provided by the multifield model is comparable to that of a fully discrete analysis, while the computational cost is much lower [3, 11].

The additional microstructural field introduced in the multifield continuum has the function of effectively smearing the microscopic heterogeneities at the macroscopic scale. More precisely, it explicitly describes the local fibre rotation and makes it possible to map the local stresses and couple stresses at the microscopic level. In this way, while the problem is solved at the coarse-grained continuum scale and the solution is obtained in terms of continuous fields defined over the body, one can easily take into account the actual microstructure. In particular, the model naturally incorporates scale parameters in the macroscopic constitutive relations, while in the classical Cauchy continuum only fibre density and aspect ratio can be accounted for.

Such features are very important for understanding the relation between the microscopic structure and the macroscopic properties of the material, and therefore for an optimum design of the microstructure itself. In fact, size and arrangement of the fibres can be properly designed in order to obtain the best performances when the material is subjected to the various loading conditions it should experience during its life time.

The present multifield–multiscale approach appears very promising for dealing with complex materials, even in a setting wider than the one presented here. For instance, in [8] a toy problem has been considered, dealing with a microcracked material containing hard inclusions. More generally, as long as the basic assumptions introduced in Sec. 1 are valid, different and complex microstructures can be easily described, and the only point one must care of concerns the description of the microstructure itself, which must be as accurate as possible. Then, the outlined multiscale strategy provides a mechanically funded basis to build up an equivalent multifield continuum endowed with the parameters suitable for describing the actual microstructure.

Acknowledgements

This work was supported in part by grants from the Italian Ministry of Instruction, University and Research (MIUR) and from the Italian Research Group in Mathematical Physics (GNFM) of the National Institute of High Mathematics (INdAM).

References

[1] Nemat-Nasser S. and Hori M. *Micromechanics: Overall Properties of Heterogeneous Materials*. Elsevier, Amsterdam, 1993.

[2] Sánchez-Palencia E. and Zaoui A. Homogenization techniques for composite media. papers from the course held in udine, july 1–5, 1985. In Snchez-Palencia

E. and Zaoui A., editors, *Lecture Notes in Physics*, volume 272. Springer-Verlag, Berlin, 1987.

[3] P. Trovalusci and R. Masiani. Non-linear micropolar and classical continua for anisotropic discontinuous materials. *Int. J. Solids Structures*, 40:1281–1297, 2003.

[4] G. Pijaudier-Cabot and Bažant Z. Nonlocal damage theory. *J. Engng. Mech, ASCE*, 113:1512–1533, 1987.

[5] L. J. Sluys, R. de Borst, and Mühlhaus H.-B. Wave propagation, localization and dispersion in a gradient-dependent medium. *Int. J. Solids Structures*, 30:1153–1171, 1993.

[6] V.G. Kouznetsova, M.G.D. Geers, W.A.M. Brekelmans. Multi-scale second-order computational homogenization of multi-phase materials: a nested finite element solution strategy. *Comput. Methods Appl. Mech. Engrg.*, 193:5525-5550, 2004.

[7] P. Trovalusci and Masiani R. Material symmetries of micropolar continua equivalent to lattices. *Int. J. Solids and Struct.*, 36:2091–2108, 1999.

[8] V. Sansalone, P. Trovalusci, and F. Cleri. Multiscale modelling of composite materials by a multifield finite element approach. *International Journal for Multiscale Computational Engineering*, 3(4):463–480, 2005.

[9] G. Capriz. *Continua with Microstructure*. Springer-Verlag, Berlin, 1989.

[10] M. Gurtin. Thermodynamics and the possibility of spatial interaction in elastic materials. *Arch. Rat. Mech. Anal.*, 19:339–352, 1965.

[11] P. Trovalusci and R. Masiani. A multifield model for blocky materials based on multiscale description. *Int. J. Solids Structures*, 42:5778–5794, 2005.

[12] W. Voigt. W. Lerbuch der Kristallphysik. *Mathematischen Wissenschaften*, XXXIV:596–616, 1910.

[13] J. L. Ericksen. Special topics in elastostatics. In C.-S. Yih, editor, *Advances in Applied Mechanics*, volume 17, pages 189–243. Academic Press, New York, 1977.

[14] V. Sansalone, P. Trovalusci, and F. Cleri. Multiscale modelling of materials by a multifield approach: Microscopic stress and strain distribution in fiber-matrix composites. *Acta Materialia*, 54(13):3485–3492, 2006.

[15] Ingomar Jäger and Peter Fratzl. Mineralized collagen fibrils: A mechanical model with a staggered arrangement of mineral particles. *Biophysical Journal*, 79(4):1737–1746, 2000.

[16] E. Cosserat and F. Cosserat. *Théorie des corps déformables*. Herman et fils, Paris, 1909.